

# SCIENTIFIC REPORTS



OPEN

## The relationship between the dislocations and microstructure in $\text{In}_{0.82}\text{Ga}_{0.18}\text{As}/\text{InP}$ heterostructures

Liang Zhao<sup>1</sup>, Zuoxing Guo<sup>1</sup>, Qiulin Wei<sup>1</sup>, Guoqing Miao<sup>2</sup> & Lei Zhao<sup>1</sup>

Received: 28 April 2016

Accepted: 20 September 2016

Published: 11 October 2016

In this work, we propose a formation mechanism to explain the relationship between the surface morphology (and microstructure) and dislocations in the  $\text{In}_{0.82}\text{Ga}_{0.18}\text{As}/\text{InP}$  heterostructure. The  $\text{In}_{0.82}\text{Ga}_{0.18}\text{As}$  epitaxial layers were grown on the  $\text{InP}$  (100) substrate at various temperatures (430 °C, 410 °C and 390 °C) using low pressure metalorganic chemical vapor deposition (LP-MOCVD). Obvious protrusions and depressions were observed on the surface of the  $\text{In}_{0.82}\text{Ga}_{0.18}\text{As}/\text{InP}$  heterostructure because of the movement of dislocations from the core to the surface. The surface morphologies of the  $\text{In}_{0.82}\text{Ga}_{0.18}\text{As}/\text{InP}$  (100) system became uneven with increasing temperature, which was associated with the formation of dislocations. Such research investigating the dislocation of large lattice mismatch heterostructures may play an important role in the future-design of semiconductor films.

As a typical III-V compound,  $\text{In}_x\text{Ga}_{1-x}\text{As}$  is one of the most important semiconductor materials<sup>1,2</sup>. Because of their excellent photoelectric properties, III-V compound films have been widely used in infrared detectors<sup>3,4</sup>, solar cells<sup>5,6</sup>, transistors<sup>2,7</sup>, optical switches<sup>8</sup> and optical fibre communications devices<sup>9</sup>. Compared to other  $\text{In}_x\text{Ga}_{1-x}\text{As}$  films, films of high-In-content semiconductor, such as  $\text{In}_{0.82}\text{Ga}_{0.18}\text{As}$ , which has a long cut-off wavelength (more than 2  $\mu\text{m}$ ) in spectroscopic applications, have attracted more attention<sup>10,11</sup>.

The methods used to prepare semiconductor films strongly influence their dislocation density and photoelectric properties, thus, various epitaxial growth technologies such as MBE<sup>12,13</sup>, SPE<sup>14</sup>, PVD<sup>15</sup> have been explored in recent years to obtain high performance semiconductor thin films. Among these main thin-film preparation method, metalorganic chemical vapor deposition (MOCVD) has been widely used in the preparation of  $\text{In}_x\text{Ga}_{1-x}\text{As}$  materials since 1968<sup>16–18</sup>.  $\text{InP}$  and  $\text{GaAs}$  are common substrates used in the fabrication of heterostructures. The lattice mismatch between the  $\text{In}_{0.82}\text{Ga}_{0.18}\text{As}$  epitaxial layer and substrate strongly affects the performance of the  $\text{In}_{0.82}\text{Ga}_{0.18}\text{As}$  films. The lattice mismatch in the  $\text{In}_{0.82}\text{Ga}_{0.18}\text{As}/\text{InP}$  heterostructure is 2%, whereas that in  $\text{In}_{0.82}\text{Ga}_{0.18}\text{As}/\text{GaAs}$  heterostructure system is greater than 5.6%<sup>19</sup>. Two-step growth<sup>20</sup> or the insertion of step-graded buffer layers between the substrate and the epitaxial layer<sup>21</sup> are common and critical approaches used to improve the quality of the epitaxial layers.

In previous studies, researchers invoked the Frank-van der Merwe, Stranski-Krastanov and Volmer-Weber growth-mode models (2D-to-3D growth-mode transition) to discuss the formation mechanism of films<sup>22–25</sup>. These models directly explain the growth process of thin films. However, the literature still contains little intuitionistic explanation about the relationship between the surface morphology and the dislocations. In our previous report, we only analysed the dislocation types (60° and 90° dislocations) at the interface in detail (the  $\text{In}_{0.82}\text{Ga}_{0.18}\text{As}$  films were prepared at 430 °C)<sup>26</sup>. As a consequence, the strain in the  $\text{In}_{0.82}\text{Ga}_{0.18}\text{As}/\text{InP}$  (100) interface was incompletely relaxed because of the formation and multiplication of misfit dislocations (MDs). Various defects including stacking faults as well as 60° and 90° threading dislocations were identified in the region near the interface, and the plastic relaxation of the strained heterostructures was obtained by the creation of MDs. The styles and the formation of the dislocations near the interface in the heterostructures have been analysed systematically in previous reports<sup>27–30</sup>.

In this work, we focused on the formation mechanism to explain the relationship between the surface morphology (and microstructure) and dislocations of  $\text{In}_{0.82}\text{Ga}_{0.18}\text{As}/\text{InP}$  heterostructure. We describe the relationship between the protrusions and depressions on the surface of the epitaxial layers. Furthermore, the movement of dislocations is further investigated. Additionally, we calculate the dislocation density in the epitaxial layers to

<sup>1</sup>Key Lab of Automobile Materials Ministry of Education, College of Materials Science and Engineering, Jilin University, Changchun, 130025, P.R. China. <sup>2</sup>State Key Laboratory of Luminescence and Applications, Changchun Institute of Optics, Fine Mechanics and Physics, Chinese Academy of Sciences, Changchun, 130033, P.R. China. Correspondence and requests for materials should be addressed to L.Z. (email: zljolly@jlu.edu.cn)

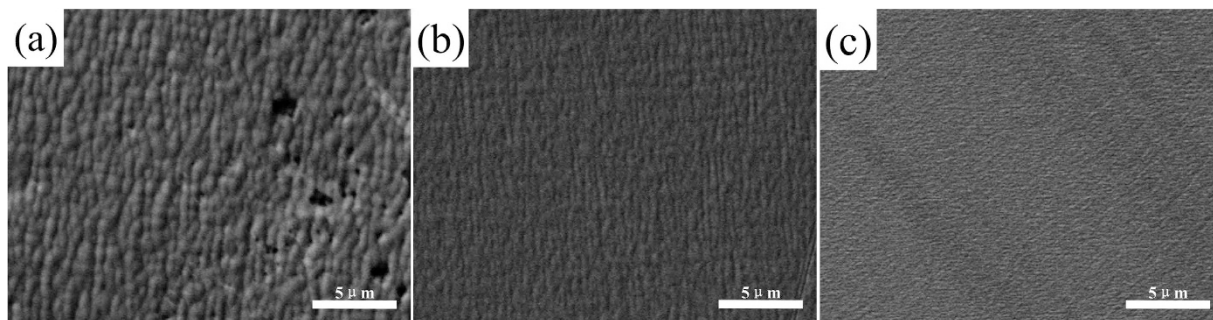


**Figure 1.** Surface morphology figures of the  $\text{In}_{0.82}\text{Ga}_{0.18}\text{As}$  layer obtained at different growth temperatures: (a) 430 °C; (b) 410 °C; (c) 390 °C.

explore the influence of the movement of dislocations on the surface morphology and the microstructure of epitaxial layers. In this paper, we emphasize our development of a formation mechanism to explain the relationship between the surface morphology (and microstructure) and the dislocations of  $\text{In}_{0.82}\text{Ga}_{0.18}\text{As}/\text{InP}$  heterostructure. To explain our model more clearly, we have included two additional experiments (at 390 °C and 410 °C) to provide better contrast with previous results.

## Results

The  $\text{In}_{0.82}\text{Ga}_{0.18}\text{As}/\text{InP}$  specimens were grown using the MOCVD (see Methods for details). The samples grown at different temperatures (430 °C, 410 °C and 390 °C) are labelled as sample A, sample B, and sample C, respectively. The surface morphologies of  $\text{In}_{0.82}\text{Ga}_{0.18}\text{As}$  layers obtained at different growth temperatures were examined by SEM; the results are shown in Fig. 1(a–c). Numerous small protrusions and depressions were observed on the surface of sample A, as shown in Fig. 1(a), and these protrusions were noticeably smaller on samples B and C, as shown in Fig. 1(b,c), respectively. Our observations demonstrate that the surface morphology became smooth as the preparation temperature was decreased. To elucidate the formation of the protrusions and depressions more clearly, we characterized the three specimens by transmission electron microscopy (TEM).

Figure 2 shows the [110] cross-section fragments of the three samples characterized by TEM. For samples A, B and C, the growth rates of the  $\text{In}_{0.82}\text{Ga}_{0.18}\text{As}$  epitaxial layer were 300, 187 and 142 nm/h at the same growth time, respectively. For samples A, B and C, shown in Fig. 2(a–c), respectively, the width of the protrusions (depressions) were approximately 520, 200 and 110 nm, whereas the heights were 90, 55 and 10 nm, respectively. These results are consistent with the SEM images in Fig. 1(a–c), respectively. The cross-section of the protrusions and the depressions on the surface arranged according to a definite principle of: depression-protrusion-depression (or protrusion-depression-protrusion); the dislocations gathered in the protrusions (depressions) shown in the red squares on the surface. The numbers of dislocations at the surface especially in the protrusions (depressions) decreased with decreasing temperature. Fig. 2(d), with blue borders, is a high resolution image at the interface of sample B (the blue square in Fig. 2(b)). Moreover, numbers of dislocations were observed at the interface because of the lattice mismatch of 2% between the  $\text{In}_{0.82}\text{Ga}_{0.18}\text{As}$  epitaxial layer and the InP substrate of each sample, as shown in Fig. 2(d).

## Discussion and Conclusion

On the basis of the aforementioned results, we propose that the surface structures are associated with the movement of the dislocations; this hypothesis can be strongly supported by calculation of the dislocation density. Usually, the full width at half maximum (FWHM) and the magnified inverse fast Fourier transform (IFFT) are used to calculate the dislocation density. The FWHM of the  $\text{In}_{0.82}\text{Ga}_{0.18}\text{As}$  epitaxial layer is an important parameter for crystalline structures examined using X-ray diffraction (XRD), according to the following formula:

$$\rho_{\text{dis}} = (\text{FWHM})^2 / 9b^2 \quad (1)$$

where  $b$  is a constant associated with the lattice parameter of  $\text{In}_{0.82}\text{Ga}_{0.18}\text{As}^{31}$ , thus, as the value of the FWHM increases, the dislocation density increases. The values are summarized in Table. 1. The XRD patterns of the InGaAs epitaxial layer and InP substrates for samples A–C are shown in Fig. 3. However, with this method, the FWHM value only reflects the average dislocation density of the epitaxial layers; we therefore calculate the dislocation density of the surface and the interface using the magnified inverse fast Fourier transform (IFFT) technique. We define the dislocation density according to the following formula:

$$\rho = n/A \quad (2)$$

where  $n$  is the number of dislocations and  $A$  is the area. On the basis of this method, the dislocation density of the interface (or the surface) can be obtained. As shown in Fig. 4, we obtained two groups of (111) half-planes on the basis of IFFT, as shown in the magnified regions of the red and blue squares, we then used Equation (2) to determine the values of the dislocation density and average the values. Using a large number of high-resolution electron microscope images, we calculated the dislocation densities of the different regions; the results are collected in Table. 1. Furthermore, from Table. 1, the dislocation density at the interface was obviously larger than

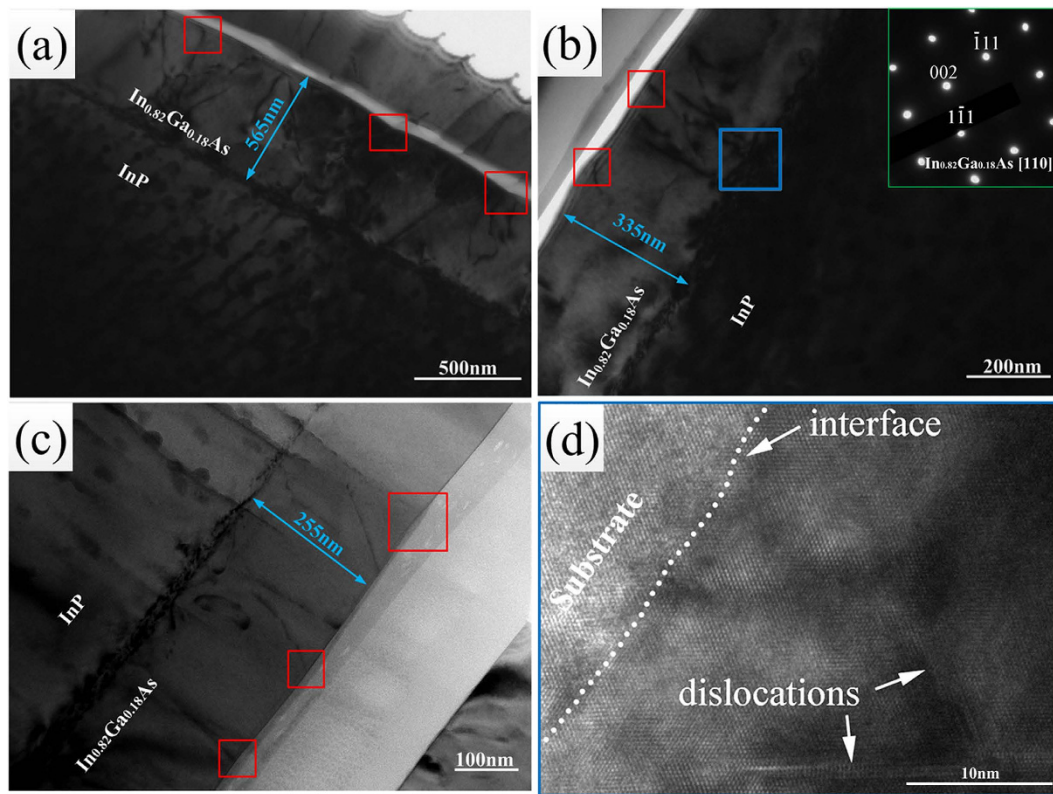


**Figure 2.** Cross-sectional views of the  $\text{In}_{0.82}\text{Ga}_{0.18}\text{As}/\text{InP}$  epitaxial layers for the [110] zone which were deposited simultaneously and at different preparation temperatures: (a) 430 °C; (b) 410 °C; (c) 390 °C.

Sample	Temperature (°C)	FWHM (degree)	$\rho_i$ ( $\text{cm}^{-2}$ )	$\rho_s$ ( $\text{cm}^{-2}$ )	$\rho_s/\rho_i$
A	430	0.489	$4.8 \times 10^{12}$	$2.5 \times 10^{12}$	45.8–65.5%
B	410	0.343	$3.7 \times 10^{12}$	$1.5 \times 10^{12}$	23.3–47.8%
C	390	0.328	$2.9 \times 10^{12}$	$0.7 \times 10^{12}$	16.2–28.1%

**Table 1.** Variation of temperature, dislocation density of the interface ( $\rho_i$ ), dislocation density of the surface ( $\rho_s$ ) and the value of  $\rho_s/\rho_i$ .

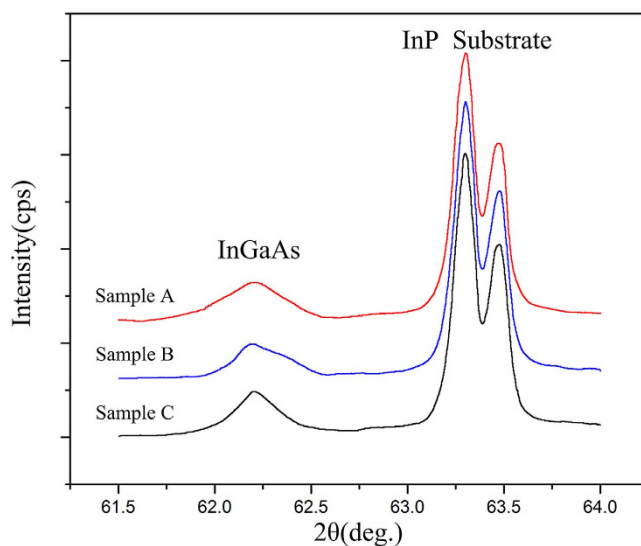


**Figure 3.** The XRD patterns of the InGaAs epitaxial layer of samples A–C.

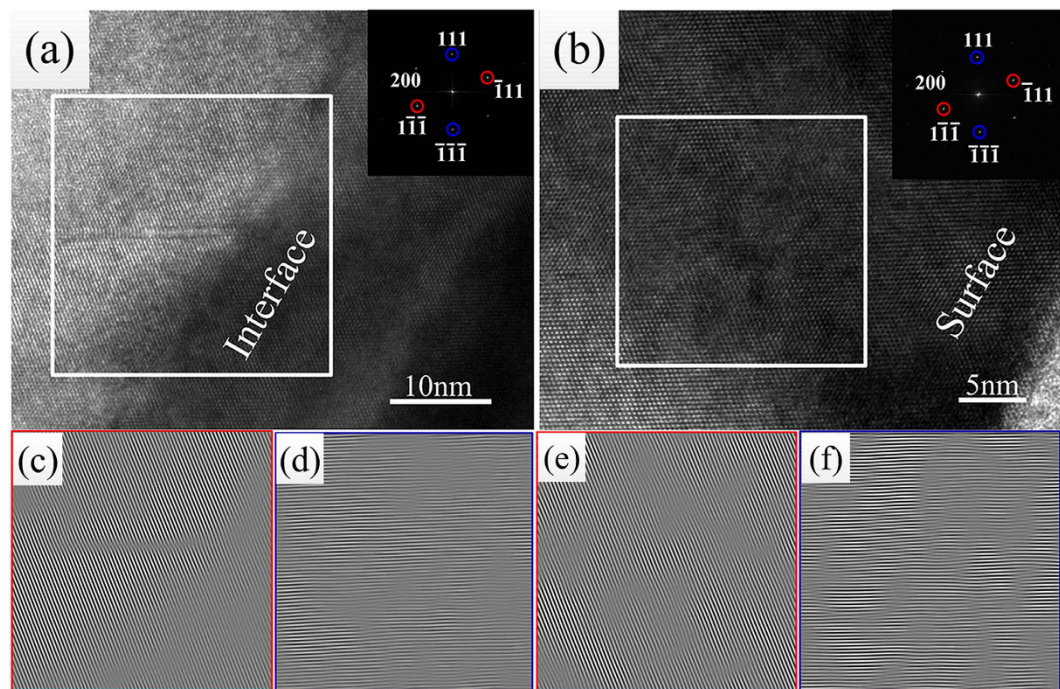


**Figure 4.** High-resolution electron microscope images and magnified inverse fast Fourier transform (IFFT) images of sample B from different regions: (a) high-resolution images at the interface; (b) high-resolution images at the surface; (c,d,e,f) IFFT images for plane groups.

that in the epitaxial layer. As the growth temperature was lowered, the dislocation densities of both the interface and the surface decreased, consistent with the trend obtained from the Equation (1). As evident for sample A, the value of  $\rho_s/\rho_i$  was 45.8–65.5%, whereas the values were 23.3–47.8% and 16.2–28.1% for sample B and sample C, respectively. These results indicate that at a higher temperature, more dislocations form and move to the surface. This observation is also consistent with the results shown in Fig. 2(a–c).

In previous reports, researchers have applied an acknowledged model in which the thin films grow via the Frank-van der Merwe, Stranski-Krastanov and Volmer-Weber growth mode (2D-to-3D growth-mode transition) to directly explain the formation mechanism of the films, as shown in Fig. 5(a). In this model, as the temperature increases, the diffusion of the atoms becomes much stronger and the strain increases; the growth of the films thus transitions from 2D growth into 3D growth to release the strain. On the basis of this model and the aforementioned analysis in this work, we here establish a simple model in which the dislocation motion in the films explains the formation mechanism of surface morphology, in cases not explained by the aforementioned model. As shown in Fig. 5(b), at the protrusions (or depressions) on the surface of heterostructure film, the dislocations lines generate together, leading to a poor surface. During the film formation process, misfit dislocations (MDs, red lines) are first formed because of the lattice mismatch in  $\text{In}_{0.82}\text{Ga}_{0.18}\text{As}/\text{InP}$  heterosystem. Second, as the film thickness increases, interaction dislocations incline towards the surface to form threading dislocations (TDs): some TDs form that depend on the dislocations' glide plane as segments (the yellow lines) and some form from the Frank–Read source (black lines)<sup>26</sup>. These TDs then propagate to the surface and result in the formation of protrusions (or depressions). At a higher growth temperature, the atomic motion becomes much stronger, and more defects, especially dislocations, are formed. When the film growth rate becomes faster, a thicker film is obtained; in a thicker film, the strain increases, resulting in the generation of more dislocations on the surface. Finally, larger and more protrusions (depressions) are formed.

In summary, the quality of the surface morphology improves and the rough surface becomes smooth with decreasing temperature. We studied the relationship between the surface morphology and the microstructure of the epitaxial layer about the dislocation motion at different temperatures. We then devised a simple model to explain the formations of films and the protrusions (or depressions) on their surface. As the film growth progresses, interaction dislocations incline form threading dislocations (TDs): some TDs form that depend on the dislocations' glide plane as segments and some form from the multiplication of the misfit dislocations (MDs). These TDs then generate on the surface and result in formation of the protrusions (or depressions). This model has the potential to be very influential in demonstrating how to use dislocations (or other defects) in the surface to improve the performance of films through surface treatments. Although the quality of our films (in terms of dislocation density) is not better than that of the films fabricated with a buffer layer, we are able to design and study how to use the dislocation of the surface to improve the surface morphology and properties, and we are able to take the epitaxial layers in this paper as the buffer layers, which represents an improvement upon the two-step growth method. Our research has the potential to play an important role in the design of semiconductor films (especially using the two-step growth method) and dislocation analysis of large lattice mismatch systems in the future.

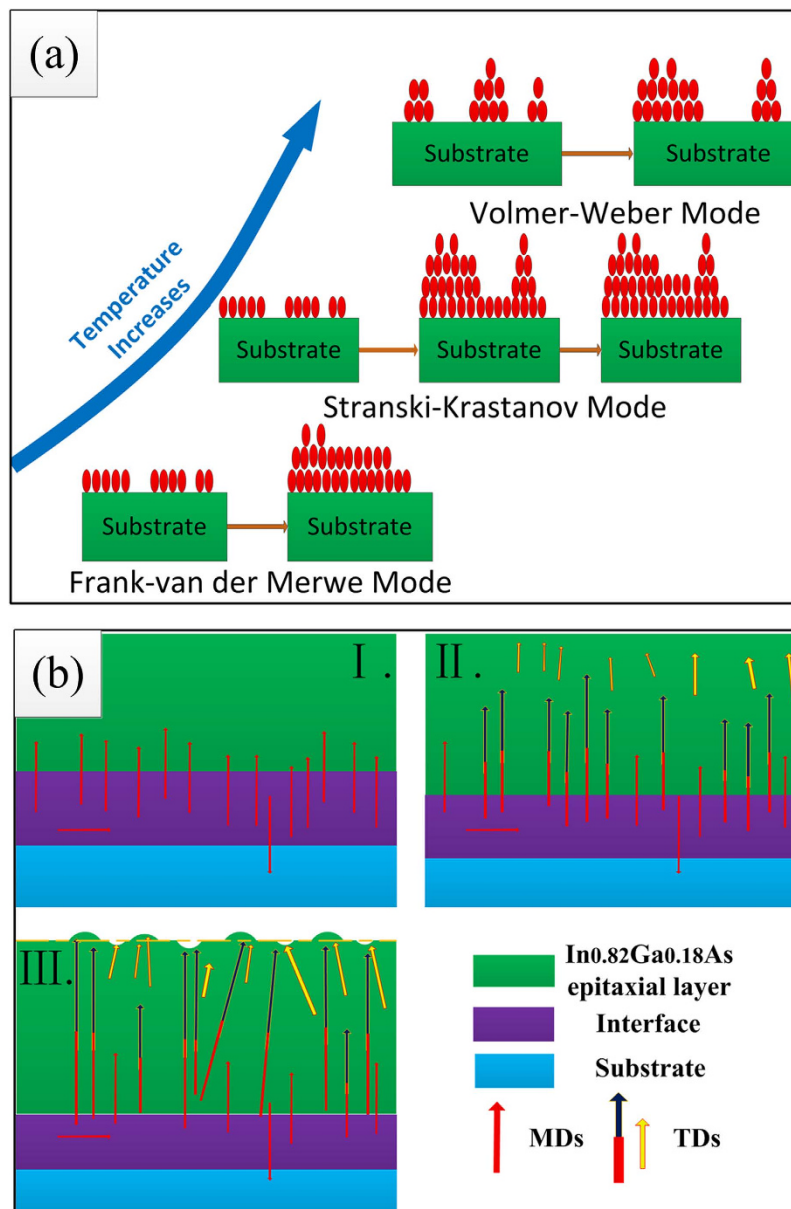


**Figure 5.** The two models of the different growth modes for the formation mechanism of films.

## Methods

**Sample preparation.** The  $\text{In}_{0.82}\text{Ga}_{0.18}\text{As}$  epitaxial layers on  $\text{InP}(100)$  were grown by low-pressure MOVCD (AIXTRON 200/4) at three different temperatures ( $430^\circ\text{C}$ ,  $410^\circ\text{C}$  and  $390^\circ\text{C}$ ), because the pyrolysis temperature of trimethylgallium (TMGa) is higher than that of Trimethylindium (TMIn). At lower temperatures, controlling indium-gallium ratio at the same growth time (90 min) to synthesize the  $\text{In}_{0.82}\text{Ga}_{0.18}\text{As}$  is difficult. In particular, at  $370^\circ\text{C}$ , the TMGa cannot be broken down<sup>32</sup>. TMGa, TMIn and 10% arsine ( $\text{AsH}_3$ ) in  $\text{H}_2$  were used as precursors. Palladium-diffused hydrogen was used as a carrier gas. The substrates on the graphite susceptor were heated under inductively coupled radio frequency power. The reactor pressure was maintained at  $1 \times 10^4$  Pa. The growth time was 90 min, and the growth rates of the  $\text{In}_{0.82}\text{Ga}_{0.18}\text{As}$  epitaxial layer were 300, 187 and 167 nm/h, respectively.

**Characterization techniques.** A high-resolution X-ray diffractometer (D8, Bruker) was used for the FWHM measurements to investigate the crystalline quality of the epitaxial layers. The surface morphology of the  $\text{In}_{0.82}\text{Ga}_{0.18}\text{As}/\text{InP}(100)$  system was detected by a scanning electron microscope (EVO-18, ZEISS). The samples for TEM observations were thinned manually and made electron-transparent by ion-milling using a Leica RES101 ion polishing system. A transmission electron microscope (JEM-2100F, JEOL) operated at 200KV was used for TEM observations; high resolution transmission electron microscopy (HRTEM) was used to observe [110] cross-section samples.

## References

- Vurgaftman, I., Meyer, J. R. & Ram-Mohan, L. R. Band parameters for III–V compound semiconductors and their alloys. *Journal of Applied Physics* **89**, 5815, doi: 10.1063/1.1368156 (2001).
- Del Alamo, J. A. Nanometre-scale electronics with III–V compound semiconductors. *Nature* **479**, 317–323 (2011).
- Tsai, C. L., Cheng, K. Y., Chou, S. T. & Lin, S. Y. InGaAs quantum wire infrared photodetector. *Applied Physics Letters* **91**, 181105, doi: 10.1063/1.2805224 (2007).
- Xia, H. *et al.* Nanoscale imaging of the photoresponse in PN junctions of InGaAs infrared detector. *Scientific reports* **6**, 21544, doi: 10.1038/srep21544 (2016).
- Pospischil, A., Furchi, M. M. & Mueller, T. Solar-energy conversion and light emission in an atomic monolayer pn diode. *Nature nanotechnology* **9**, 257–261 (2014).
- Geisz, J. F. *et al.* High-efficiency GaInP/GaAs/InGaAs triple-junction solar cells grown inverted with a metamorphic bottom junction. *Applied Physics Letters* **91**, 023502, doi: 10.1063/1.2753729 (2007).
- Wang, P.-F. *et al.* A Semi-floating gate transistor for low-voltage ultrafast memory and sensing operation. *science* **341**, 640–643 (2013).
- Wang, S. *et al.* MOVPE growth of grade-strained bulk InGaAs/InP for broad-band optoelectronic device applications. *Journal of Crystal Growth* **260**, 464–468, doi: 10.1016/j.jcrysgro.2003.09.003 (2004).
- Kim, J. *et al.* Misfit dislocation generated in InAs epilayer and InP substrate interfaces grown by metalorganic chemical-vapor deposition. *Materials Letters* **53**, 446–451 (2002).
- Zhang, Y. *et al.* Wavelength extended 2.4 $\mu$ m heterojunction InGaAs photodiodes with InAlAs cap and linearly graded buffer layers suitable for both front and back illuminations. *Infrared Physics & Technology* **51**, 316–321, doi: 10.1016/j.infrared.2007.09.003 (2008).
- Li, C. *et al.* Distinction investigation of InGaAs photodetectors cutoff at 2.9 $\mu$ m. *Infrared Physics & Technology* **53**, 173–176, doi: 10.1016/j.infrared.2009.11.002 (2010).
- Gao, F. *et al.* Achieving high-quality In<sub>0.3</sub>Ga<sub>0.7</sub>As films on GaAs substrates by low-temperature molecular beam epitaxy. *CrystEngComm* **16**, 10774–10779, doi: 10.1039/c4ce01558d (2014).
- Zhang, Z. Y. *et al.* 1.55 microm InAs/GaAs quantum dots and high repetition rate quantum dot SESAM mode-locked laser. *Scientific reports* **2**, 477, doi: 10.1038/srep00477 (2012).
- Suzumura, I. *et al.* Nucleation and growth of Ge on Si (111) in solid phase epitaxy. *Thin Solid Films* **369**, 116–120 (2000).
- Speliotis, T. *et al.* Effect of deposition pressure and post deposition annealing on SmCo thin film properties. *physica status solidi (c)* **5**, 3759–3762 (2008).
- Manasevit, H. M. Single-Crystal Gallium Arsenide on Insulating Substrates. *Applied Physics Letters* **12**, 156, doi: 10.1063/1.1651934 (1968).
- Wood, C. *et al.* Terahertz emission from metal-organic chemical vapor deposition grown Fe: InGaAs using 830 nm to 1.55  $\mu$ m excitation. *Applied Physics Letters* **96**, 194104 (2010).
- Byrnes, D. P., Ebert, C., Pulwin, Z., Krahnert, A. & Ramos, F. In *Photovoltaic Specialist Conference (PVSC)*, IEEE 40th. 1135–1138 (IEEE) (2014).
- Chang, S.-Z., Chang, T.-C. & Lee, S.-C. The growth of highly mismatched In<sub>x</sub>Ga<sub>1-x</sub>As (0.28  $\leq x \leq 1$ ) on GaAs by molecular-beam epitaxy. *Journal of Applied Physics* **73**, 4916, doi: 10.1063/1.353809 (1993).
- Li, J., Miao, G., Zhang, Z. & Zeng, Y. Experiments and analysis of the two-step growth of InGaAs on GaAs substrate. *CrystEngComm* **17**, 5808–5813, doi: 10.1039/c5ce00979k (2015).
- Wang, T. Y., Ou, S. L., Horng, R. H. & Wu, D. S. Growth evolution of Si x N y on the GaN underlayer and its effects on GaN-on-Si (111) heteroepitaxial quality. *CrystEngComm* **16**, 5724–5731 (2014).
- Samonji, K., Yonezu, H., Takagi, Y. & Ohshima, N. Evolution process of cross-hatch patterns and reduction of surface roughness in (InAs)<sub>m</sub>(GaAs)<sub>n</sub> strained short-period superlattices and InGaAs alloy layers grown on GaAs. *Journal of Applied Physics* **86**, 1331, doi: 10.1063/1.370891 (1999).
- Medel-Ruiz, C. I. *et al.* In situ monitoring of the 2D–3D growth-mode transition in In<sub>0.3</sub>Ga<sub>0.7</sub>As/GaAs (001) by reflectance-difference spectroscopy. *Applied Surface Science* **221**, 48–52, doi: 10.1016/s0169-4332(03)00957-7 (2004).
- Leonard, D., Krishnamurthy, M., Reaves, C. M., Denbaars, S. P. & Petroff, P. M. Direct formation of quantum-sized dots from uniform coherent islands of InGaAs on GaAs surfaces. *Applied Physics Letters* **63**, 3203, doi: 10.1063/1.110199 (1993).
- Krzyzewski, T., Joyce, P., Bell, G. & Jones, T. Role of two- and three-dimensional surface structures in InAs-GaAs (001) quantum dot nucleation. *Physical Review B* **66**, 121307 (2002).
- Zhao, L., Sun, J. G., Guo, Z. X. & Miao, G. Q. TEM dislocations characterization of In<sub>x</sub>Ga<sub>1-x</sub>As/InP (100) (x = 0.82) on mismatched InP substrate. *Materials Letters* **106**, 222–224, doi: 10.1016/j.matlet.2013.04.116 (2013).
- Chen, Y. *et al.* Dislocation formation mechanism in strained In<sub>x</sub>Ga<sub>1-x</sub>As islands grown on GaAs (001) substrates. *Applied physics letters* **68**, 111–113 (1996).
- Chu, S. N. G., Macrander, A. T., Strege, K. E. & Johnston, W. D. Misfit stress in InGaAs/InP heteroepitaxial structures grown by vapor-phase epitaxy. *Journal of Applied Physics* **57**, 249, doi: 10.1063/1.334797 (1985).
- Narayan, J. & Oktyabrsky, S. Formation of misfit dislocations in thin film heterostructures. *Journal of Applied Physics* **92**, 7122, doi: 10.1063/1.1521789 (2002).
- Mathis, S. K., Chavarkar, P., Andrews, A. M., Mishra, U. K. & Speck, J. S. Strain relaxation of InGaAs by lateral oxidation of AlAs. *Journal of Vacuum Science & Technology B: Microelectronics and Nanometer Structures* **18**, 2066, doi: 10.1116/1.1303739 (2000).
- Liu, X. *et al.* Influence of thermal annealing duration of buffer layer on the crystalline quality of In<sub>0.82</sub>Ga<sub>0.18</sub>As grown on InP substrate by LP-MOCVD. *Applied Surface Science* **257**, 1996–1999, doi: 10.1016/j.apsusc.2010.09.041 (2011).
- Yoshida, M., Watanabe, H. & Uesugi, F. Mass Spectrometric Study of Ga (CH<sub>3</sub>)<sub>3</sub> and Ga (C<sub>2</sub>H<sub>5</sub>)<sub>3</sub> Decomposition Reaction in H<sub>2</sub> and N<sub>2</sub>. *Journal of the Electrochemical Society* **132**, 677–679 (1985).

## Acknowledgements

The authors gratefully acknowledge financial support from the National Nature Science Foundation (No. 61474053), the National Key Basic Research Project of China (973 Project, No. 2012CB619200), the 2014 Natural Science Basic Research Open Foundation of the Key Lab of Automobile Materials, Ministry of Education, Jilin University (No. 1018320144001) and the State Key Laboratory for Mechanical Behavior of Materials (No. 20161806).

## Author Contributions

Z.G. designed the project and guided the research. G.M. carried out the preparation of the In<sub>0.82</sub>Ga<sub>0.18</sub>As/InP. Q.W. prepared the samples for TEM observations. Liang Z. and Lei Z. conducted SEM, TEM and HRTEM observations and wrote the paper. Z.G. and G.M. revised the paper. All authors contributed to the discussions.

### Additional Information

**Competing financial interests:** The authors declare no competing financial interests.

**How to cite this article:** Zhao, L. *et al.* The relationship between the dislocations and microstructure in  $\text{In}_{0.82}\text{Ga}_{0.18}\text{As}/\text{InP}$  heterostructures. *Sci. Rep.* **6**, 35139; doi: 10.1038/srep35139 (2016).



This work is licensed under a Creative Commons Attribution 4.0 International License. The images or other third party material in this article are included in the article's Creative Commons license, unless indicated otherwise in the credit line; if the material is not included under the Creative Commons license, users will need to obtain permission from the license holder to reproduce the material. To view a copy of this license, visit <http://creativecommons.org/licenses/by/4.0/>

© The Author(s) 2016